HHS Public Access

Author manuscript

J Biomed Mater Res A. Author manuscript; available in PMC 2019 October 07.

Published in final edited form as:

J Biomed Mater Res A. 2018 August ; 106(8): 2251–2260. doi:10.1002/jbm.a.36411.

Effects of Antigen Removal on a Porcine Osteochondral Xenograft for Articular Cartilage Repair

Steve Elder[1], **Hudson Chenault**[1], **Paul Gloth**[1], **Katie Webb**[1], **Ruth Recinos**[1], **Emily Wright**[1], **Dalton Moran**[1], **James Butler**[2], **Abdolsamad Borazjani**[3], **Avery Cooley**[4]

[1]Department of Agricultural & Biological Engineering, James Worth Bagley College of Engineering, Mississippi State University, Starkville, MS

[2]Department of Clinical Sciences, College of Veterinary Medicine, Mississippi State University, Starkville, MS

[3]Department of Basic Sciences, College of Veterinary Medicine, Mississippi State University, Starkville, MS

[4]Department of Pathobiology and Population Medicine, College of Veterinary Medicine, Mississippi State University, Starkville, MS

Abstract

Given the limited availability of fresh osteochondral allografts and uncertainty regarding performance of decellularized allografts, this study was undertaken as part of an effort to develop an osteochondral xenograft for articular cartilage repair. The purpose was to evaluate a simple antigen removal procedure based mainly on treatment with SDS and nucleases. Histology demonstrated a preservation of collagenous structure and removal of most nuclei. Immunohistochemistry revealed the apparent retention of α-Gal within osteocyte lacunae unless the tissue underwent an additional α-galactosidase processing step. Cytoplasmic protein was completely removed as shown by Western blot. Quantitatively, the antigen removal protocol was found to extract approximately 90% of DNA from cartilage and bone, and it extracted over 80% of glycosaminoglycan from cartilage. Collagen content was not affected. Mechanical testing of cartilage and bone were performed separately, in addition to testing the cartilage-bone interface, and the main effect of antigen removal was an increase in cartilage hydraulic permeability. *In vivo* immunogenicity was assessed by subcutaneous implantation into DBA/1J mice, and the response was typical of a foreign body rather than immune reaction. Thus an osteochondral xenograft produced as described has the potential for further development into a treatment for osteochondral lesions in the human knee.

Keywords

osteochondral xenograft; antigen removal; α-Gal; biomechanics; immunogenicity

Corresponding Author: Dr. Steven Elder, Department of Agricultural & Biological Engineering, P.O. Box 9632, Mississippi State, MS 39762, Phone: (662) 325-9107, selder@abe.msstat.edu.

Introduction

Among cartilage repair procedures, osteochondral autograft transfer and osteochondral allograft transplantation provide immediate restoration of mature functional cartilage to the joint surface and offer the highest rates of return to sporting activities[1]. The major limitations of autograft transfer are the relatively small amount of tissue available for harvest and risk of donor site morbidity [2]. Limitations of osteochondral allograft transplantation include low supply and short shelf life. The tissue must come from a young donor within 24 hours of death, and should be transplanted within 28 days of harvest for the highest likelihood of a successful outcome[3]. The window of transplantation is further narrowed by the need to perform testing for bacterial, fungal, and viral contamination prior to release. A decellularized osteochondral allograft implant with a 24-month shelf life was designed to overcome the fresh allograft shortage problem. However, a recent prospective review of 32 decellularized graft recipients followed for up to 2.8 years revealed a 72% failure rate [4].

With the aim of improving on such outcomes, we seek to develop an acellular osteochondral xenograft for articular cartilage repair. The ideal xenograft would retain the ECM structure but be free of antigens. In addition, mechanical properties of graft cartilage would match those of the surrounding host cartilage. Furthermore, the ideal graft would facilitate integration with adjacent tissue, as well as promote regeneration of host cartilage and bone at the same rate as the graft is degraded. While antigen removal is quite feasible, the other goals are more challenging. For example, loss of compressive stiffness seems to be an unavoidable side effect of efficient cartilage decellularization [5,6,7], and failure of grafted cartilage to integrate with host tissue is a persistent problem in cartilage tissue engineering [8]. Nonetheless, we hypothesize that the desirable properties can be achieved through efficient antigen removal followed by crosslinking, immobilization of chemotactic and/or chondrogenic factors, and perhaps incorporation of intraoperatively isolated stem cells. The potential for an osteochondral xenograft crosslinked through photooxidation to remain mechanically stable and achieve satisfactory joint congruency for up to 12 months in a sheep model has been demonstrated previously [9]. This promising outcome was achieved despite the lack of decellularization, which is generally considered essential to successful outcomes following implantation of xenograft-derived scaffolds [10]. Our previous research has demonstrated that the mechanical properties and enzymatic resistance of decellularized porcine cartilage can be modulated through treatment with plant-derived chemical crosslinking agents[11,7]. However, the effects of decellularization alone were not fully described.

The current study was undertaken to characterize the effects of dellularization on a porcine osteochondral xenograft to establish a baseline scaffold suitable for enhancement through crosslinking, growth factor functionalization, and autologous cell seeding. The antigen removal protocol under study is appealing for its simplicity. Relying primarily on sodium dodecyl sulfate (SDS) and nucleases, it does not involve repetitive freeze/thaw cycles, osmotic shock, strong acids or bases, high pressure/vacuum, or processing at temperatures other than ambient and 37 °C. Removal of cells and their associated nucleic acids and proteins is of primary importance for avoiding an adverse immune reaction (inflammation) and for minimizing the risk of transmitting xenopathogens and transgenes. Removal of the

α-Gal epitope (Galα1–3Galβ1–4GlcNAc-R) is a secondary consideration [12]. The α-Gal epitope can be found on cell surface glycolipids and glycoproteins in all mammals apart from Old World monkeys, apes, and humans. Humans produce anti-Gala antibody, and the binding of anti-Gal antibody to the α-Gal epitope is responsible for hyperacute rejection of pig organs transplanted into humans [13]. Although the presence of α-Gal may not preclude a graft from serving as a scaffold for tissue remodeling, it has been shown to alter the host response and warrants examination [12,14,15,16]

Our approach to osteochondral xenograft development utilizes pigs as the donors. The pig was selected because of its widespread availability, its rapid growth rate, the ease of obtaining stifle joints as byproducts of meat processing, and similarity in overall size and cartilage thickness to humans [17]. Other studies of osteochondral xenografts have involved the use of bovine tissue [5,6]. These investigations have shown that treatment of bovine osteochondral explants with SDS and nucleases can efficiently remove cells and DNA while preserving collagen content. They have also demonstrated that the decellularized tissue displays minimal cytotoxicity. A negative side effect of efficient antigen removal was the loss of glycosaminoglycan from cartilage and a reduction in compressive stiffness [5,6]. Our laboratory has made similar observations using porcine cartilage, and we have evaluated the use of natural crosslinking agents such as genipin and epigallocatechin gallate (EGCG) to increase xenograft enzymatic resistance and enhance the mechanical properties [11,7]. Results suggest that crosslinking porcine cartilage from which substantial glycosaminoglycan (GAG) has been extracted can completely restore its compressive resistance. Thus the purpose of this study is to thoroughly characterize the effects of an SDS/nuclease-based antigen removal protocol on the biochemical, biomechanical, and biological properties of a porcine osteochondral scaffold.

Materials and Methods

All reagents were purchased from Sigma-Aldrich (St. Louis, MO) unless otherwise specified. Stifle joints of approximately 6 month old pigs were obtained from a local abattoir.

Antigen Removal

Cylindrical osteochondral plugs, 5 mm diameter × ~8 mm, were harvested from the femoral condyles and patellofemoral grooves. Cleaning and decellularization was accomplished by incubating plugs in the following solutions (20 plugs in 50 ml of solution per batch):

1. Remove superficial marrow and blood: Phosphate buffered saline (PBS), 1 hour
2. Remove interstitial marrow and blood: 3% hydrogen peroxide, 6 hours; solution changed every 2 hours
3. Degrease: Chloroform:methanol (1:1), 1.5 hours
4. Methanol, 0.5 hours
5. Distilled water, 1 hour; solution changed after 0.5 hours

6. Break down cytoplasmic and nuclear membranes, digest cytoplasmic proteins, remove DNA and RNA, extract GAG: 10 mM Tris-HCl (pH 7.6), 1 mM phenylmethylsulfonyl fluoride (PMSF), 2% wt/vol SDS, 5 mM $MgCl_2$, 0.5 mM $CaCl_2$, 0.5 mg/ml DNase I, 0.05 mg/ml RNase, 1% v/v antibiotic-antimycotic mixture for 48 hours; solution changed after 24 hours
7. Distilled water, 3 hours, solution changed every hour
8. Sterilize: 2% peracetic acid/ethanol/distilled water (2:1:1), 4 hours
9. Remove residual peracetic acid and equilibrate in PBS; solution changed until the peroxide concentration in wash solution was less than 1 mg/liter as measured by test stick (Quantofix Peroxide 100, Macherey-Nagel Inc., Bethlehem, PA)

All steps were carried out under orbital shaking at 37 °C (MaxQ 4000, Thermo Scientific, Marietta, OH), except for steps 1, 8, and 9, which were carried out at room temperature. For the α-Gal immunohistochemistry experiment, some tissue underwent an additional processing step after the SDS treatment. Those plugs were incubated for 4 hours at 37 °C in 25U/ml α1–3,6 galactosidase (New England BioLabs, Ipswich, MA), 50 mM sodium acetate (pH 5.5), 5 mM $CaCl_2$, and 0.01% wt/vol bovine serum albumin (BSA).

Histology and α-Gal Immunohistochemistry (IHC)

All histology and IHC procedures were carried out on sections from three different osteochondral plugs in each group. Fresh and decellularized plugs were fixed in 10% neutral buffered formalin. Paraffin embedded sections were stained with fast green/safranin-O to demonstrate GAG in the extacellular matrix and counterstained with hematoxylin to show cell nuclei. Additional sections were stained with hematoxylin and picrosirius red to display collagen. Images were captured on a Leica DM2500 microscope equipped with DFC420 C camera (200X). Residual α-Gal was detected using fluorescence immunohistochemistry. Antigen retrieval and blocking were carried out by sequential incubation in 0.1% pronase (15 minutes at 37 °C) and 10% horse serum (30 minutes at room temperature). M86 murine monoclonal primary antibody (Enzo Life Sciences, Farmingdale, NY) was diluted in PBS containing 1% BSA to 15 μg/ml, and sections were incubated overnight at 4 °C. The secondary antibody, anti-mouse immunoglobulin M–fluorescein isothiocyanate (IgM-FITC), was diluted in PBS/10% BSA to 25 μg/ml and applied for 2 hours at room temperature. Red marrow cells in the fresh sections served as positive controls, and specificity was tested by substituting antibody diluent for the primary antibody during staining of fresh sections. Sections were counterstained with propidium iodide and imaged on a Zeiss 510 confocal scanning microscope with green and red filter sets.

Western Blot

Residual vimentin, a marker of cytoplasmic protein, was detected by sodium dodecyl sulfate-polyacrylamide gel electrophoresis (SDS-PAGE) and immunoblotting (two independent samples from each group). Cartilage and bone were analyzed separately. In addition to the full antigen removal procedure specified above, some samples were treated with SDS and nucleases (step 6 above) for only 6 hours. Freeze-dried tissue was weighed and homogenized in lysis buffer consisting of 10 mM Tris (pH 7.4), 100 mM NaCl, 1 mM

ethylenediaminetetraacetic acid (EDTA), 1 mM ethylene glycol tetraacetic acid (EGTA), 1 mM PMSF, 1% Triton X-100, 10% glycerol, 0.1% SDS, and 0.5% deoxycholate (approximately 30 mg in 3 ml of lysis buffer). Sample volumes were adjusted to contain equal amounts of tissue by dry weight. Extracted proteins were denatured by boiling for 5 minutes in Laemmli buffer containing β-mercaptoethanol. Protein samples and a Li-Cor WesternSure® Pre-stained Chemiluminescent Protein Ladder were separated by electrophoresis in 10% Mini-PROTEAN® TGX™ Precast Protein Gels (Bio-Rad, Hercules, CA) and transferred to PVDF membranes using a Trans-Blot® SD Semi-Dry Transfer Cell (Bio-Rad). Membranes were blocked with 5% non-fat dry milk and immunoblotted with mouse monoclonal antibody to vimentin (0.42 μg/ml, AMF-17b, Developmental Studies Hybridoma Bank, Iowa City, IA), followed by horseradish peroxidase-conjugated goat anti-mouse secondary antibody (0.067 μg/ml, Bio-Rad). Enhanced chemiluminescence (SuperSignal™ West Pico Chemiluminescent Substrate, ThermoFisher Scientific, Waltham, MA) and a ChemiDoc XRS+ imaging system (Bio-Rad) were used for development and protein visualization. Relative band intensity was quantified using the gel analysis tools in ImageJ [18].

Biochemistry

For measurement of DNA and characterization of the cartilage extracellular matrix (n = 12 per group), cartilage and bone were separated, freeze dried, and digested in 100 mM sodium phosphate buffer/10 mM Na_2EDTA/10 mM L-cysteine/0.125 mg/mL papain overnight at 60 °C. DNA was analyzed by fluorescence assay using bisBenzimide (DNAQF, Sigma). Fluorescence was read using a Glomax Multi Jr Detection System (Promega, Madison, WI). DNA content was quantified by comparison to a standard curve generated using known amounts of calf thymus DNA. Cartilage GAG content was determined using the Blyscan Glycosaminoglycan Assay based on binding to dimethylmethylene blue dye (Biocolor, Carrickfergus, County Antrim, UK). Precise quantities were determined from a standard curve developed using the chondroitin sulphate supplied with the kit. Cartilage collagen content was determined using the chloramine-T hydroxyproline assay according to Reddy and Enwemeka [19]. Colorimetric results were obtained using a μQuant Microplate Spectrophotometer (Biotek, Winooski, VT). Hydroxyproline was used to develop a standard curve, and the amount of collagen was calculated assuming 12.5% of collagen is hydroxyproline. DNA, GAG, and collagen contents were normalized to tissue dry weight.

Mechanical Testing

All tissue for mechanical testing underwent the same number of freeze/thaw cycles. Fresh controls were frozen immediately after harvest, while experimental samples were processed as described above and then frozen. Individual samples were thawed to room temperature on the day of testing. The biphasic properties of cartilage were determined from curve-fitting results of a uniaxial, confined compression creep test to the linear biphasic model of Mow et al. [20]. Full-thickness cartilage disks of 5 mm diameter (n = 12 per condition) were pressed into an impermeable cylindrical chamber with diameter of 4.7 mm. The chamber was part of a custom apparatus similar to the one utilized for creep testing by Soltz and Ateshian [21]. A porous indenter of 4.3 mm diameter was settled onto the tissue for a period of 1 hour under a load of 1.1 N (0.07 MPa). An additional test load of 1.8 N (0.1 MPa) was then applied for a

period of 3 hours, during which time the displacement of the indenter was continuously measured at 0.1 Hz sampling rate. Curve fitting by the method of least squares to find the aggregate modulus, H_A, and permeability, k_0, was performed using Microsoft Excel, as was calculation of the coefficient of determination, r^2 [21].

The effect of antigen removal on compressive resistance of bone was determined by unconfined compression testing (n = 9 per group). Osteochondral cores of 6 mm diameter × 15 mm were harvested using a cylindrical chisel (Single Use OATS Set, Arthrex, Naples, FL). Prior to testing, all samples were trimmed using a small kerf hobby saw to remove cartilage and square the ends. The testing machine was a 2K Electromechanical Universal Testing System with 890 N (200 lb) load cell (MTI, Marietta, GA). After applying a preload of 5 N, bone cylinders were compressed between smooth, impermeable platens at a constant rate of 1 mm/min until failure. Young's modulus was calculated as the slope of the linear region of the stress versus strain curve, which was typically in the range of 3–5% strain. Energy of distortion was calculated as the area under the stress-strain curve up to the point of maximum stress.

Strength of the cartilage-bone interface was evaluated by shear testing in the same machine. Osteochondral plugs of 5 mm diameter (n = 12 per condition) were grouted in polymethyl methacrylate (PMMA) cement in 1.5 ml microcentrifuge tubes. The cartilage was cut sharply along the diameter and half the cartilage removed by cutting as close to the bone as possible. This exposed a rectangular shelf of cartilage 5 mm × cartilage thickness. The PMMA-embedded bone and cartilage shelf were aligned perpendicular to the axis of the testing machine and clamped in place so that a broad, flat ram attached to the actuator could slide against the exposed bone, barely touching. The ram was advanced at 0.1 mm/sec until failure of the cartilage-bone interface. Stiffness was calculated as the slope of the linear region of the force-displacement curve. Strength was taken as the maximum load. Work to failure was calculated as the area under the force-displacement curve until the maximum force.

In vivo Immunocompatibility

An in vivo experiment in mice was undertaken following a protocol approved by Mississippi State University Institutional Animal and Care and Use Committee (16–009). Osteochondral plugs 6mm in diameter × ~7mm were harvested from a porcine distal femur using a circular chisel (Arthrex). Following antigen removal and sterilization as described above, a single xenograft was implanted into each of four 7-week old male DBA/1J mice (The Jackson Laboratory, Bar Harbor, ME). Under isoflurane anesthesia, each mouse received a xenograft placed subcutaneously in a midline cranio-dorsal pocket that was closed using two 4–0 polydioxanone (PDS) monofilament sutures. Mice were allowed food and water ad libitum for 12 weeks, at which time they were humanely euthanized using carbon dioxide. Grafts and surrounding tissue were dissected en bloc, fixed in 10% neutral buffered formal, and embedded in paraffin. Sections were stained with hematoxylin and eosin and evaluated by a pathologist.

Statistical Analysis

Quantitative data were analyzed by two-sample independent t-test ($\alpha = 0.05$) using IBM SPSS Statistics 23.

Results

Antigen removal processing yielded a bleached construct with cartilage remaining firmly attached to bone. The cartilage retained a macroscopically smooth surface, and its indentation resistance was palpably less than that of normal articular cartilage. Representative histology results are shown in figures 1 and 2. In fresh cartilage positive safranin-O staining for GAG increased in intensity with depth from the articular surface. It was absent only in the top few micrometers. Antigen removal abolished all positive staining for safranin-O except in calcified cartilage. Antigen removal also eliminated almost all positive hematoxylin staining for cell nuclei; nearly all the lacunae of treated cartilage and bone were empty. Qualitatively, collagen content appears not to have been affected by antigen removal as there was little difference in picrosirius red staining intensity between fresh and treated cartilage.

Positive immunostaining for α-Gal in fresh tissue was associated with osteocytes and marrow cells. It was not detected in cartilage or in sections from which the primary antibody had been omitted (data not shown). In the bone, α-Gal was located at the cell surface of osteocytes (Fig. 3). Although the multi-step antigen removal process, including SDS and nucleases, removed cell nuclei as indicated by lack of propidium iodide staining, it did not remove α-Gal. Prominent staining for α-Gal persisted at the periphery of bone lacunae after antigen removal. However, all positive staining for α-Gal was abolished by a 4-hour treatment with 25 U/ml α1–3,6 galactosidase.

Western blot results for cartilage and bone were very similar. In fresh tissue, vimentin was detected as a high-intensity band with a size of approximately 44 kDa (Fig. 4). No vimentin was detectable after antigen removal in either cartilage or bone, except for in one bone sample which displayed 1.4% band density relative to the average control after 6 hours of SDS treatment. As shown in Table 1, antigen removal processing extracted approximately 90% of the DNA from cartilage and bone, and reduced the GAG content of cartilage by over 80%. Collagen content was nearly the same in control and decellularized cartilage.

Results of confined compression testing on articular cartilage are shown in Figure 5. In all cases r^2 was ≥ 0.91. With respect to aggregate modulus, there was not a statistically significant difference between control and decellularized cartilage ($p = 0.12$). However, hydraulic permeability of cartilage treated with the antigen removal procedure was significantly greater than the permeability of control cartilage by an average of 84% ($p = 0.04$). The properties of bone in unconfined compression are summarized in Table 2. Variability was rather high in both groups, and there were no statistically significant differences between them. Regarding the cartilage-bone interface, statistically significant effects of antigen removal were not observed with respect to stiffness (8.84 ± 3.71 N/mm for controls vs. 8.50 ± 3.54 N/mm for treated, $p = 0.82$), strength (11.00 ± 4.18 N for controls vs. 7.82 ± 3.73 N for experimental, $p = 0.070$), or work to failure (8.78 ± 4.42 N-mm for

controls vs. 5.61 ± 3.92 N-mm for experimental, $p = 0.085$). However, it should be noted that statistically significant differences may only become apparent at a much a higher sample size due to considerable variability.

In all experimental animals the skin healed over the implanted xenografts and the hair had grown back within 12 weeks. At the time of retrieval, the skin was tight around the grafts and no redness or swelling was observed. Xenografts elicited predominantly a histiocytic response, typical of a foreign body rather than a sustained immune reaction as would be indicated by a lymphocytic infiltrate with epithelioid macrophages, and plasma cells indicating antibody formation and a humoral response. The bulk of the grafts remained intact and portions of the cartilage surface were undisturbed and covered by a thin layer of proliferative mesenchymal cells (Fig. 6a). In some areas, particularly on the cut edges, a weak inflammatory response was evidenced by chondrolysis and gradual cellular invasion of the lytic spaces with fibrovascular tissue and inflammatory cells, macrophages and neutrophils (Fig. 6b,c). However, the maximum depth of cell penetration was not more than 200 μm. Virtually no inflammatory response occurred in central marrow spaces in the bone; medullary spaces were filled almost entirely by fibrovascular tissue and significant osteolysis was not observed (Fig. 6d,e). Focal mild reactive inflammation and osteolysis was limited to marginal medullary spaces and trabeculae (Fig. 6f).

Discussion

The ultimate aim of our research is to develop an osteochondral xenograft alternative to autografts and allografts for repair of osteochondral lesions. Based on our own experience and the reports of others, it is not possible to achieve efficient antigen removal without significant disruption of the cartilage extracellular matrix [11,7,5,6]. We therefore believe that collagen crosslinking following antigen removal is needed to restore compressive resistance and protect against rapid enzymatic degradation. While our previous research pertained to the effects of crosslinking [11,7], the current study is focused on characterizing the effects of a simple approach to antigen removal. It involves cleaning in hydrogen peroxide to remove blood and marrow, degreasing in chloroform:methanol, treating with SDS to solubilize membranes (cytoplasmic and nuclear) and cytoplasmic proteins, and use of nucleases to remove DNA and RNA. The final step is sterilization by peracetic acid.

Xenografts contain antigens which are recognized as foreign by a patient’s immune system and will thus induce an inflammatory response. DNA removal is important for avoiding an adverse immune reaction to xenogenic material [22,23]. Commercially available ECM-derived biologic scaffolds have been shown to contain some antigenic epitopes and residual DNA, the presence of which can lead to chronic inflammation, fibrosis, scarring, and encapsulation [24]. In addition, residual DNA could transmit xenopathogens and transgenes. In order to avoid adverse cell and host response to a decellularized construct, Crapo et al. have recommended that nuclear material be undetectable in tissue sections stained with hematoxylin and eosin and that residual DNA not exceed 50 ng per mg ECM dry weight [25]. The antigen removal protocol presented herein met these criteria with respect to bone and fell just short with respect to cartilage. While bone lacunae were completely empty, small nuclear fragments were occasionally observed in cartilage lacunae. Quantitatively,

residual DNA in bone was < 50 ng/mg on dry weight basis (34.5), but in cartilage it was > 50 ng/mg (127.9 ng/mg dry weight). Residual DNA in cartilage was higher than the previously measured 39.7 ng/mg in bovine cartilage after an antigen removal procedure developed by Fermor and coworkers [6]. Nonethelss, our protocol removed 89% of the native DNA, and we speculate that a further reduction could be achieved simply by extending the duration of nuclease treatment and the number of washing steps that follow.

A thorough evaluation of antigen removal should go beyond quantification of DNA [10]. This study includes examination of the cytoplasmic protein vimentin and the α-Gal epitope (Galalpha1–3Galbeta1-(3)4GlcNAc-R). Vimentin is a major component of a eukaryotic cell's cytoskeleton and was used as a marker of abundant cytoplasmic proteins. Alpha-Gal is a carbohydrate moiety present on the cell surface in all mammals except Old World monkeys and humans. In pig-to-human xenotransplantation, rejection occurs mainly as a result of the α-Gal epitope remaining on the porcine cell surface. In humans, the α-Gal gene is mutated, and the moiety is not expressed. However, humans have circulating immunoglobulins with specificity for cell surface α-Gal. A previous study of porcine xenograft menisci transplanted into monkeys demonstrated a vigorous immune response to α-Gal epitopes including activation of many B lymphocytes and increased production of anti-Gal IgG which could lead to chronic rejection of xenografts [26]. Western blotting demonstrated that all vimentin was digested by the SDS treatment. This finding is similar to the complete removal of another cytoplasmic protein, β-actin, by 22-hour treatment with SDS as previously measured in human umbilical artery [27]. In fresh osteochondral tissue positive staining for α-Gal around osteocyte lacunae and bone marrow cells, as well as the absence of staining in bone matrix and cartilage, were consistent with previous reports of α-Gal distribution [5,28]. It is apparent that the antigen removal protocol without galactosidase is ineffective at eliminating α-Gal. This observation is consistent with the detection of α-Gal in bovine pericardium after treatment with 1% SDS [29]. Fortunately, a 4-hour treatment with galactosidase appears to efficiently remove α-Gal from bone similar to the loss of α-Gal expression from porcine veins that has been shown to occur within 30 minutes [30]. Although the effects of galactosidase on the cartilage and bone ECM were not measured, there is no reason to suspect that such a mild enzymatic treatment would affect the primary collagen and mineral components.

The degree of antigen removal resulting from the SDS/nuclease protocol under study was adequate to prevent a chronic immune response to subcutaneously implanted xenografts in a collagen-sensitive mouse model. Xenografts elicited a mild foreign body reaction characterized by invasion of fibrovascular tissue in the bone marrow space and a thin fibroblastic encapsulation of cartilage. Of course it is possible that there could have been a more mixed inflammatory cell infiltrate at an earlier point that rapidly abated due to lack of necessity for an antigen-driven cellular or humoral immune response. Although the bulk of the xenograft cartilage remained intact, some remodeling activity was evident at specific sites along the periphery. Galactosyl transferase knock out mice were found to respond in a similar fashion to porcine cartilage decellularized by a more aggressive protocol that involved freeze-thaw cycles and osmotic shock in addition to treatment with SDS and nucleases [5]. As in the current study, a fibrous capsule was found to surround decellularized explants, a response that was observed to fresh osteochondral porcine tissue as well. The

response to fresh tissue also included vacuolation and loss of structural integrity, phenomena not seen in response to the decellularized grafts tested in the current study. In addition, similar patterns of cell concentration at the periphery of decellularized implants with occasional burrowing of mononuclear and fibroblast-like cells into the interior were observed in both studies. This reaction can be considered to represent a tissue remodeling response [5].

Like others, the antigen removal protocol under study extracts the majority of GAG. Removal of GAG is advantageous for increasing porosity and facilitating invasion by host stem cells or chondrocytes and for enhancing delivery of nutrients and removal of metabolic waste products [31,32]. Without GAG extraction, cultured human chondrocytes were found to attach to cartilage explants, but they were not able to migrate into the tissue within 28 days [33]. Human primary nasal septal chondrocytes seeded onto GAG-free decellularized porcine nasal septal cartilage explants were found to migrate progressively deeper within the explant up to 42 days, by which time nearly the entire 1mm thick construct contained newly synthesized aggrecan [32]. A similar infiltration of GAG-free decellularized bovine cartilage occurred within 6 weeks of implantation in rabbit knees [31]. There is some speculation that glycosaminoglycans, because they can interact with cytokines and chemokines, might be antigenic [34]. Indeed, purified xenogeneic cartilage ECM components have been shown to provoke an immune response, and GAG extraction could reasonably be expected to decrease immunogenicity [35]. GAG removal may even improve the integration of the xenograft with surrounding host cartilage. Hyaluronidase and collagenase treatment of wounded bovine cartilage significantly improved the histological integration and biomechanical bonding strength after subcutaneous implantation in nude mice [36].

The loss of GAG increased hydraulic permeability of cartilage, but it did not significantly affect the aggregate modulus, suggesting that the antigen removal procedure left the cartilage network largely intact. Picrosirius red staining for collagen in tissue sections and collagen content determined by chloramine-T assay for hydroxyproline also indicate a negligible effect of the antigen removal procedure on cartilage collagen. Our previous research demonstrates that the compressive resistance of GAG-depleted cartilage can be increased in a predictable manner to physiological levels and above through collagen crosslinking, for example by genipin [11,7]. The antigen removal procedure did not significantly affect the compressive properties of the cancellous bone. It also did not substantially weaken the cartilage-bone interface, failure of which appears to factor significantly into the low success rate of decellularized osteochondral allografts [4]. Osteochondral allografts were susceptible to loss of the cartilage cap. Cartilage-bone interfacial shear strength in adult humans has been reported to be 7.25±1.35 MPa [37], a much higher strength than reported herein for adolescent porcine tissue (0.80±0.38 MPa after normalization to the estimated area of cartilage-bone contact). However, we have demonstrated that collagen crosslinking, an additional processing step to be included in the production of xenografts intended for in vivo applications, increases cartilage-bone interfacial strength [38]. In a study performed in our laboratory, porcine osteochondral xenografts decellularized by a method similar to the one under study were implanted in 13 rabbits, and there were no cases of cartilage-bone delamination and loss of graft cartilage

after 16 weeks (data not shown). Assessing the true risk of osteochondral xenograft cartilage loss requires a long-term trial in a large animal model.

In conclusion, the simple protocol described in this study efficiently removes the antigenic components of porcine osteochondral tissue, provided that treatment with galactosidase is included. Regarding its overall impact on the extracellular matrix of the osteochondral construct, our results indicate that the effects of antigen removal are minimal with the exception of GAG loss and increase in cartilage hydraulic permeability. The collagenous structure and other mechanical properties are preserved. Excessive residual DNA in cartilage remains a concern if following the protocol as presented, but we speculate that minor adjustments can increase DNA removal without additional detrimental effects to the cartilage and bone ECM. Nonetheless, decellularized porcine osteochondral plugs twelve weeks after subcutaneous implantation in collagen-sensitive mice were found to elicit only a mild chronic inflammatory response typical of a foreign body such as suture material. Therefore, porcine osteochondral tissue processed according to the antigen removal method presented herein appears to be suitable for further development into a treatment for osteochondral lesions in the human knee.

Acknowledgments

Research reported in this publication was supported by the National Institute of Arthritis and Musculoskeletal and Skin Diseases of the National Institutes of Health under Award Number R15AR066926. The content is solely the responsibility of the authors and does not necessarily represent the official views of the National Institutes of Health. Additional support was provided by the Mississippi State University Office of Research and Economic Development.

References

1. Krych A, Pareek A, King A, Johnson N, Stuart M, Williams R. Return to sport after the surgical management of articular cartilage lesions in the knee: a meta-analysis. Knee Surg Sports Traumatol Arthrosc. 2017;25(10)3186–3196. [PubMed: 27539401]
2. Treme G, Miller M. Autograft osteochondral transfer. Oper Tech Sports Med. 2008;16:81–88.
3. Nuelle C, Nuelle J, Cook J, Stannard J. Patient factors, donor age, and graft storage duration affect osteochondral allograft outcomes in knees with or without comobidities. J Knee Surg. 2017;30(2): 179–184. [PubMed: 27228198]
4. Farr J, Gracitelli G, Shah N, Chang EY, Gomoll A. High failure rate of a decellularized osteochondral allograft for the treatment of cartilage lesions. Am J Sports Med. 2016;44(8):2015–22. [PubMed: 27179056]
5. Kheir E, Stapleton T, Shaw D, Jin Z, Fisher J, Ingham E. Development and characterization of an acellular porcine cartilage bone matrix for use in tissue engineering. J Biomed Mater Res A. 2011;99A(2):283–294.
6. Fermor H, Russell S, Williams S, Fisher J, Ingham E. Development and characterization of a decellularised bovine osteochondral biomaterial for cartilage repair. J Mater Sci: Mater Med. 2015;26(5):186. [PubMed: 25893393]
7. Elder S, Pinheiro A, Young C, Smith P, Wright E. Evaluation of genipin for stabilization of decellularized porcine cartilage. J Orthop Res. 2017;35(9):1949–1957. [PubMed: 27859554]
8. Doran P. Cartilage Tissue Engineering: What Have We Learned in Practice? Methods Mol Biol. 2015;1340:3–21. [PubMed: 26445827]
9. von Rechenberg B, Akens M, Nadler D, et al. Mosaicplasty with photooxidized, mushroom shaped, bovine, oteochondral xenografts in experimental sheep. Vet Comp Orthop Traumatol. 2006;19:147–56. [PubMed: 16971997]

10. Cissell D, Hu J, Griffiths LG, Athanasiou K. Antigen removal for the production of biomechanically functional, xenogeneic tissue grafts. Journal of Biomechanics. 2014;47(9):1987–96. [PubMed: 24268315]
11. Pinheiro A, Cooley A, Liao J, Prabhu R, Elder S. Comparison of natural crosslinking agents for stabilization of xenogenic articular cartilage. Journal of Orthopaedic Research. 2016;34(6):1037–1046. [PubMed: 26632206]
12. Raeder R, Badylak S, Sheehan C, Kallakury B, Metzger D. Natural anti-galactose alpha 1,3 galactose antibodies delay, but do not prevent the acceptance of extracellular matrix xenografts. Transplant Immunology. 2002;10(1):15–24. [PubMed: 12182460]
13. Sandrin M, McKenzie I. Gal alpha (1,3)Gal, the major xenoantigen(s) recognised in pigs by human natural antibodies. Immunol Rev. 1994;141:169–90. [PubMed: 7532618]
14. Kim M, Jeong S, Lim H, Kim Y. Differences in xenoreactive immune response and patterns of calcification of porcine and bovine tissues in alpha-Gal knock-out and wild-type mouse implantation models. Eur J Cardiothorac Surg. 2015;48(3):392–9. [PubMed: 25549993]
15. Xu H, Wan H, Zuo W, et al. A porcine-derived acellular dermal scaffold that supports soft tissue regeneration: removal of terminal galactose-alpha-(1,3)-galactose and retention of matrix structure. Tissue Eng Part A. 2009;15(7):1807–19. [PubMed: 19196142]
16. Stone K, Ayala G, Goldstein J, Hurst R, Walgenback A, Galili U. Porcine cartilage transplants in the cynomolgus monkey. III. Transplantation of alpha-galactosidase-treated porcine cartilage. Transplantation. 1998;65(12):1577–83. [PubMed: 9665073]
17. Wayne J, Brodrick C, Mukherjee N. Measurement of articular cartilage thickness in the articulated knee. Annals of Biomedical Engineering. 1998;26:96–102. [PubMed: 10355554]
18. Rasband W ImageJ, U.S. National Institutes of Health, Bethesda, Maryland, USA 1997–2016 Available at: https://imagej.nih.gov/ij/.
19. Reddy G, Enwemeka C. A simplified method for the analysis of hydroxyproline in biological tissues. Clinical Biochemistry. 1996;29(3):225–229. [PubMed: 8740508]
20. Mow V, Kuei S, Lai W, Armstrong C. Biphasic creep and stress relaxation of articular cartilage in compression: theory and experiments. J Biomech Eng. 1980;102(1):73–84. [PubMed: 7382457]
21. Soltz M, Ateshian G. Experimental verification and theoretical prediction of cartilage interstitial fluid pressurization at an impermeable contact interface in confined compression. Journal of Biomechanics. 1998;31:927–934. [PubMed: 9840758]
22. Zheng M, Chen J, Kirilak Y, Willers C, Xu J, Wood D. Porcine small intestine submucosa (SIS) is not an acellular collagenous matrix and contains porcine DNA: possible implications in human implantation. J Biomed Mater Res B Appl Biomater. 2005;73:61–67. [PubMed: 15736287]
23. Gilbert T, Freund J, Badylak S. Quantification of DNA in biological scaffold materials. J Surg Res. 2009;152(1):135–139. [PubMed: 18619621]
24. Valentin J, Badylak J, McCabe G, Badylak S. Extracellular matrix bioscaffolds for orthopaedic applications. A comparative histologic study. J Bone Joint Surg Am. 2006;88(12):2673–86. [PubMed: 17142418]
25. Crapo P, Gilbert T, Badylak S. An overview of tissue and whole organ decellularization processes. Biomaterials. 2011;32(12):3233–43. [PubMed: 21296410]
26. Galili U, LaTemple D, Walgenbach A, Stone K. Porcine and bovine cartilage transplants in cynomolgus monkey: II. Changes in anti-Gal response during chronic rejection. Transplantation. 1997;63(5):646–651. [PubMed: 9075832]
27. Gui L, Chan S, Breuer C, Niklason L. Novel utilization of serum in tissue decellularization. Tissue Engineering: Part C. 2010;16(2):173–184.
28. Feng W, Lian Y, Zhou Z, et al. Distribution of the alpha-gal epitope on adult porcine bone tissue. Transplant Proc. 2006;38(7):2247–51. [PubMed: 16980056]
29. Wong M, Wong J, Athanasiou K, Griffiths L. Stepwise solubilization-based antigen removal for xenogeneic scaffold generation in tissue engineering. Acta Biomaterialia. 2013;9:6492–6501. [PubMed: 23321301]
30. Luo Y, Wen J, Luo C, Cummings R, Cooper D. Pig xenogeneic antigen modification with green coffee bean alpha-galactosidase. Xenotransplantation. 1999;6(4):238–48. [PubMed: 10704067]

31. Toolan B, Frenkel S, Pereira D, Alexander H. Development of a novel osteochondral graft for cartilage repair. J Biomed Mater Res. 1998;41:244–250. [PubMed: 9638529]
32. Schwarz S, Elsaesser A, Koerber L, et al. Processed xenogenic cartilage as innovative biomatrix for cartilage tissue engineering: effects on chondrocyte differentiation and function. J Tissue Eng Regen Med. 2015;9(12):E239–51. [PubMed: 23193064]
33. Secretan C, Bagnall K, Jomha N. Effects of introducing cultured human chondrocytes into a human articular cartilage explant model. Cell Tissue Res. 2010;339:421–427. [PubMed: 20012649]
34. Rieder E, Seebacher G, Kasimir MT, et al. Tissue engineering of heart valves. Circulation. 2005;111:2792–2797. [PubMed: 15911701]
35. Friedlaender G, Ladenbauer-Bellis I, Chrisman O. Immunogenicity of xenogeneic cartilage matrix components in a rabbit model. Yale J Biol Med. 1983;56(3):211–7. [PubMed: 6419482]
36. van de Breevaart Bravenboer J, In der Maur C, Bos P, et al. Improved cartilage integration and interfacial strength after enzymatic treatment in a cartilage transplantation model. Arthritis Res Ther. 2004;6(5):R469–76. [PubMed: 15380046]
37. Kumar P, Oka M, Nakamura T, Yamamuro T, Delecrin J. Mechanical strength of osteochondral junction. Nihon Seikeigeka Gakkai Zasshi. 1991;65(11):1070–1. [PubMed: 1761907]
38. Elder S, Clune J, Walker J, G P. Suitability of EGCG as a means of stabilizing a porcine osteochondral xenograft. Journal of Functional Biomaterials. 2017;8(4):E43. [PubMed: 28946629]

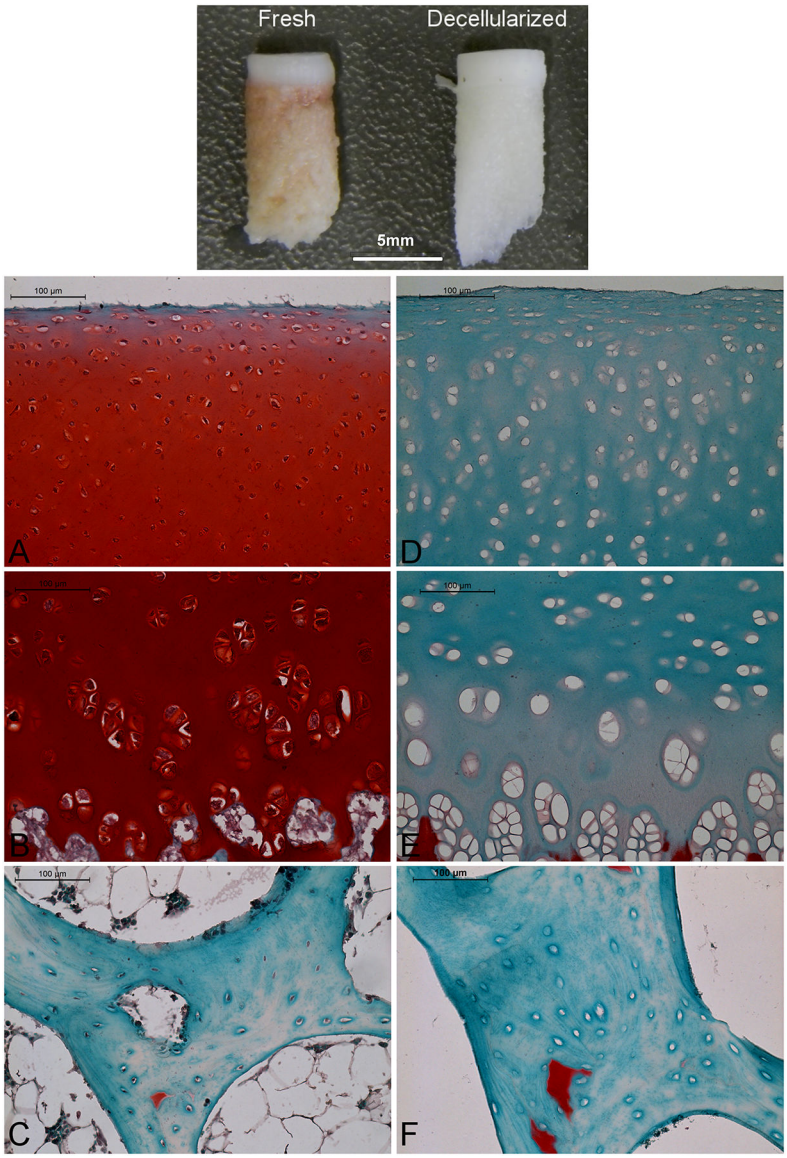

Figure 1.

Effect of antigen removal on porcine articular cartilage and subchondral bone. Top panel – macroscopic appearance (scale bar = 5 mm). Panels A-D: microscopic appearance after staining with fast green/safranin-O and hematoxylin to demonstrate glycosaminoglycan and cell nuclei, respectively. A-C – native; D-F – decellularized; A,D – superficial/transition zone of cartilage; B,E – deep zone of cartilage; C,F – Bone. Red = proteoglycan, Blue = fibrous matrix, Black = cell nuclei. A-D scale bars = 100 μm.

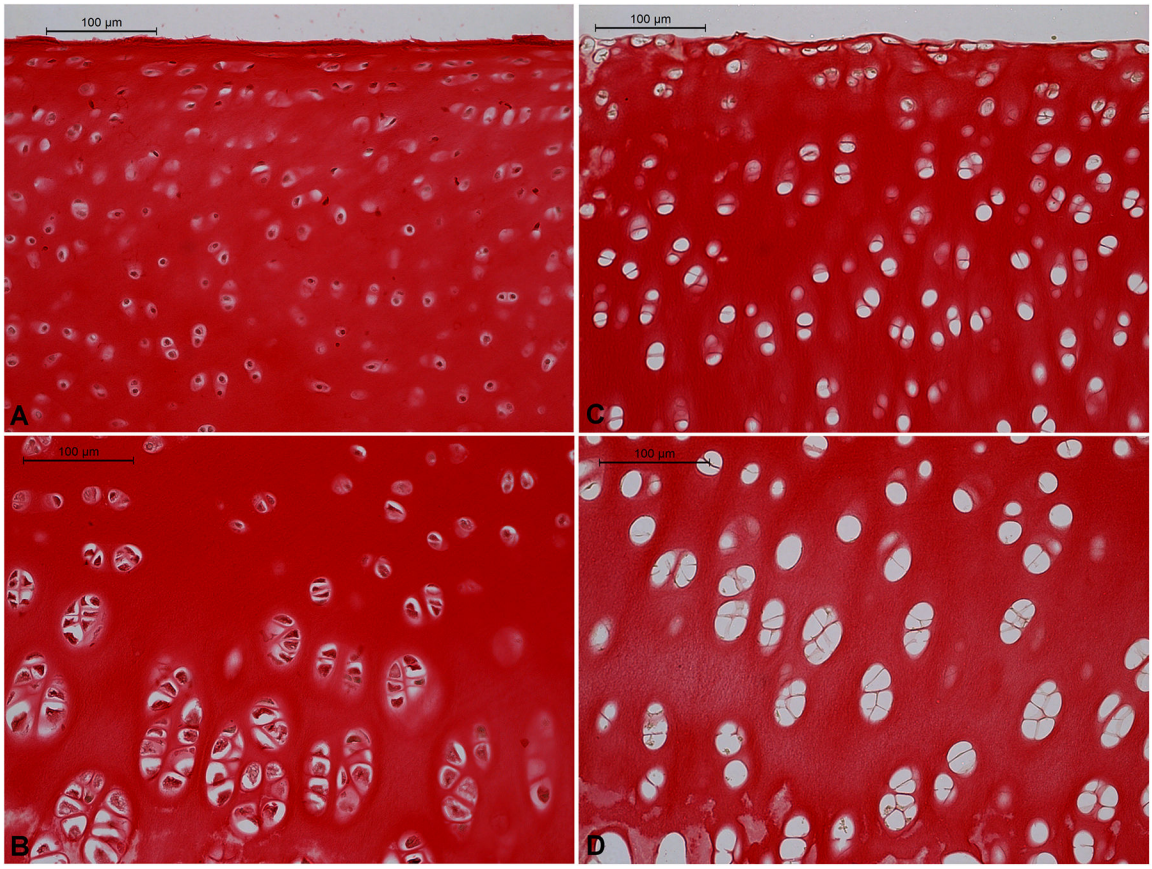

Figure 2.

Effect of antigen removal on collagen content of cartilage as indicated by picrosirius red and hematoxylin staining. A,B – native; C,D – decellularized; A,C – superficial/transition zone; B,D – deep zone. Red = collagen, Brown/Black = cell nuclei. Scale bars = 100 μm.

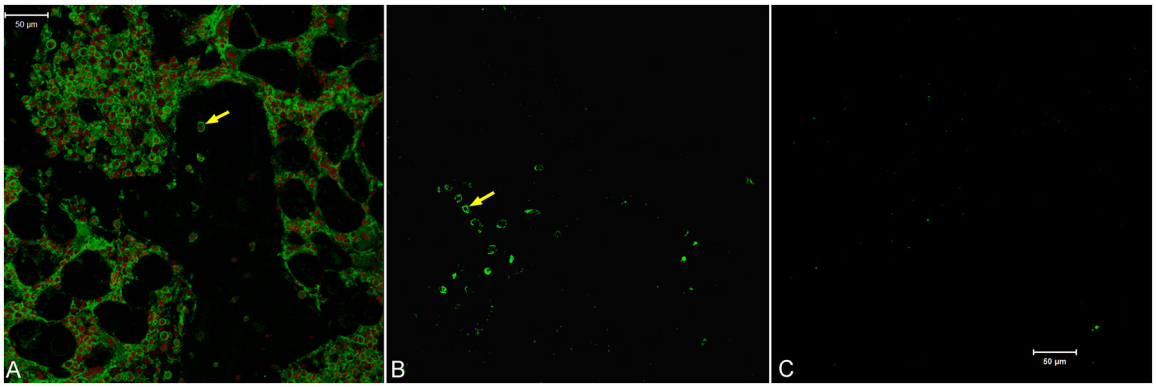

Figure 3.

Effect of antigen removal on residual α-Gal in porcine bone. Arrows indicate positive staining for α-Gal at the periphery of lacunae in fresh bone (A) as well as bone treated with SDS and nucleases (B). No positive staining was observed when antigen removal included an additional galactosidase treatment step (C). Green = α-Gal, Red = cell nuclei. Scale bars = 50 μm.

Figure 4.

Effect of antigen removal on residual vimentin in cartilage and bone. Each sample was isolated from different pieces of tissue. Cartilage: Lanes 1,2 – native tissue samples; Lanes 3,4 – decellularized cartilage samples with step 6 of antigen removal procedure truncated to 6 hours; Lanes 5,6 – decellularized cartilage samples with step 6 was carried out for 48 hours as specified in the protocol; Lane 7 – empty; Lane 8 – MW marker. Bone: Lane 1 – MW marker; Lane 2 – empty; Lanes 3,4 – decellularized bone samples with step 6 was carried out for 48 hours as specified in the protocol; Lanes 5,6 – decellularized bone samples with step 6 of antigen removal procedure truncated to 6 hours; Lanes 7,8 – native tissue samples.

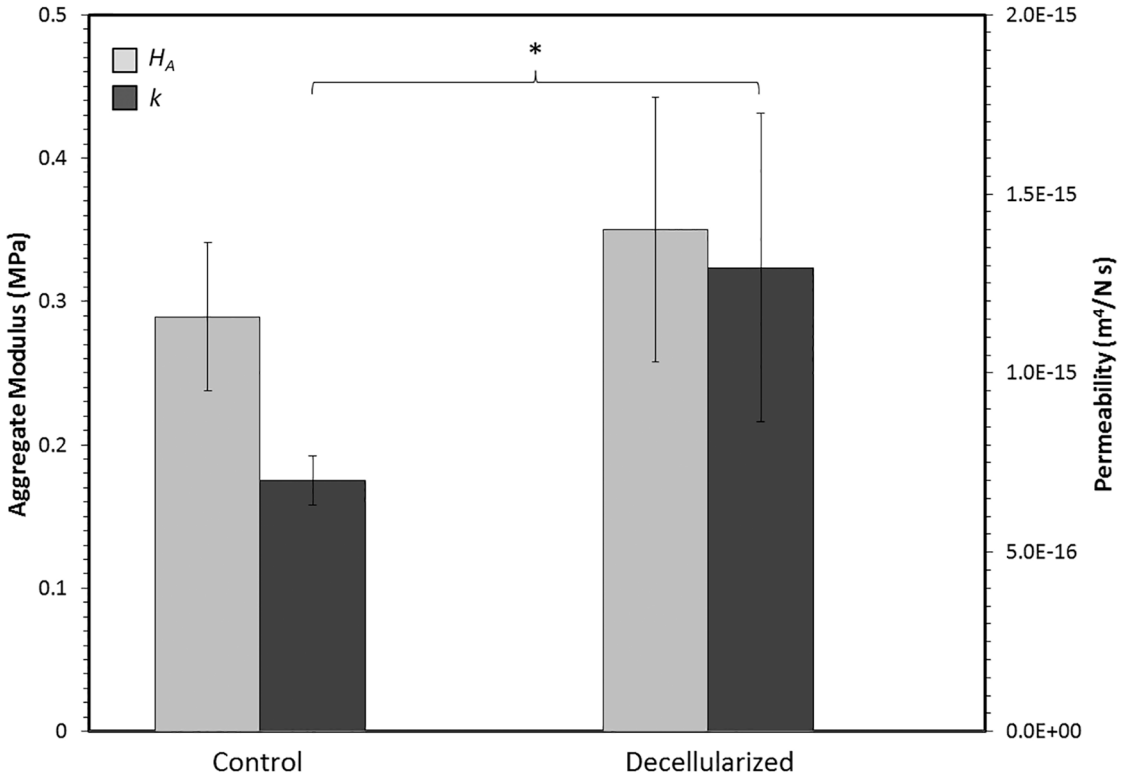

Figure 5.
Effect of antigen removal on the biphasic properties of articular cartilage derived from creep curve-fitting. Asterisk indicates a statistically significant difference.

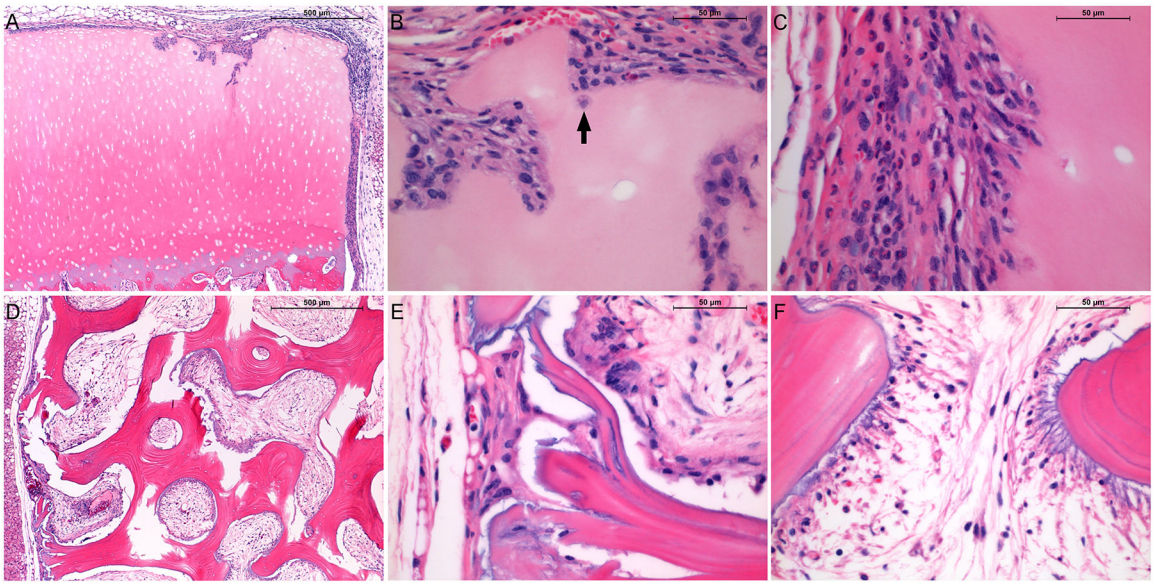

Figure 6.

Hematoxylin and eosin-stained sections of decellularized porcine osteochondral xenografts 12 weeks after subcutaneous implantation in 7-week old DBA/1J mice. A – xenograft cartilage/host interface; B – xenograft cartilage articular surface (arrow indicates infiltrating macrophage); C – xenograft cartilage cut surface; D – xenograft bone/host interface (50X); E – xenograft bone periphery; F – xenograft bone interior. Red/Pink = eosinophilic proteins including extracellular matrix and cell cytoplasm, Blue = basophilic structures including cell nuclei. A,D scalebars = 500 μm; B,C,E,F scalebars = 50 μm.

Table 1.

Effect of decellularization on DNA and ECM content of porcine osteochondral tissue (mean ± standard deviation).

	Control		Decellularized	
	Cartilage	**Bone**	**Cartilage**	**Bone**
DNA (ng/mg dry weight)	1163.5 ± 258.3	415.7 ± 137.7	127.9 ±29.8 *	34.5 ± 8.0 *
Collagen (μg/mg dry weight)	191.6 ± 42.1	Not measured	190.5 ± 44.2	Not measured
GAG (μg/mg dry weight)	94.1 ± 9.6	Not measured	15.6 ± 3.6 *	Not measured

* Significant difference with respect to control ($p<0.05$)

Table 2.

Effect of Decellularization on the Mechanical Properties of Bone in Unconfined Compression (Mean ± Standard Deviation).

	Control	**Decellularized**	***p*-value**
Young's Modulus (MPa)	198.2 ± 159.5	144.9 ± 101.3	0.41
Maximum Stress (MPa)	11.8 ± 6.0	11.9 ± 6.5	0.92
Distortion Energy to Maximum Stress (N-mm/mm^3)	6.2 ± 2.1	7.0 ± 4.1	0.62